Open access • Journal Article • DOI:10.1109/JLT.1983.1072087

Depolarization in a single-mode optical fiber — Source link

W. Burns, R. Moeller, Chin-Lin Chen

Institutions: United States Naval Research Laboratory

Published on: 01 Mar 1983 - Journal of Lightwave Technology (IEEE)

Topics: Polarization-maintaining optical fiber, Graded-index fiber, Dispersion-shifted fiber, Single-mode optical fiber and Photonic-crystal fiber

Depolarization in a Single-Mode Optical Fiber

WILLIAM K. BURNS, MEMBER, IEEE, ROBERT P. MOELLER, AND CHIN-LIN CHEN

Abstract—**The reduction of the degree of polarization of broad-band light due to propagation in ordinary single-mode fiber is examined theoretically and experimentally. Previous work is extended to account for polarization-mode coupling along the fiber by developing a model for one discrete mode-coupling center and extending it qualitatively to include multiple centers. The existence of nonzero degree of polarization in long lengths of fiber is shown to be due to mode coupling at particular positions along the fiber and the degree of polarization is shown to be related to the degree of coherence associated with the mode-coupling site. The experimental results generally support the model developed.**

I. INTRODUCTION

THE DEGREE OF POLARIZATION, defined as the fraction of optical power that is polarized, will be an important quantity in optical-fiber applications that involve interference, such as coherent communications and sensors. Rashleigh and Ulrich [1] pointed out that the different group velocities associated with the polarization modes of ordinary single-mode fibers lead to the depolarization of broad-band sources. This effect will occur to some extent with any source, depending on the group-delay difference and the fiber length. Although in communications depolarization is likely to be undesirable, recent fiber-optical gyroscope experiments [2], [3], with broad-band sources have indicated that depolarization is useful in reducing noise in the signal. We are primarily interested in this latter limit here.

A recent theoretical treatment [4] on this subject provides a general expression for the degree of polarization in an anisotropic single-mode fiber as a function of the degree of coherence, associated with the fiber and source, and the input conditions. However, this treatment cannot be applied to experimental results in many cases where power transfer or mode coupling between the polarization modes takes place. This phenomenon, which degrades the performance of high birefringence or polarization-holding fibers, has been described theoretically by Kaminow [5] with a random coupling model which was recently experimentally confirmed [6]. Mode coupling plays an important role in determining the degree of polarization in single-mode fibers. Indeed, the experiment by Rashleigh *et al.* [6] depended on depolarization subsequent to mode coupling for achieving a reliable measurement. Our work is closely related to this except that we focus on lower birefringence, ordinary single-mode fiber, where complete depolarization does not occur.

In this paper, we extend theoretically the work of Sakai *et al.* [4] to include the effect of one discrete mode-coupling center. We then show experimentally that this simple model, with some qualitative modification to account for multiple centers, can account for most of the observed behavior of depolarization in a single-mode fiber with a broad-band source. In particular, we show that mode-coupling centers at particular locations in the fiber are responsible for the absence of complete depolarization in long lengths of lower birefringence fiber. The reduction of the degree of polarization from its input value is shown to be essentially complete over a length that corresponds to the characteristic distance for polarization-mode mixing, as one might expect from the high birefringence results [6]. These results provide additional insight into the process of optical depolarization in single-mode fibers of low or high birefringence.

II. THEORY

We consider a single-mode fiber with linear birefringence so there are two well-defined polarization modes with differing phase and group velocities. If each mode is excited equally by a polarized broad-band source, the differential group velocity can lead to depolarization in a length which depends on the source bandwidth and the fiber-group-delay difference [1]. We are interested in cases where this depolarization length is short compared to the fiber length. Depolarization occurs because the differential group delay becomes greater than the coherence time of the source. To accumulate this much differential group delay, the interfering optical components must experience different group velocities over a fiber length equal to, or greater than, the depolarization length. We can intuitively construct a physical picture whereby mode-coupling centers which couple the polarization modes (Fig. 1) can frustrate this condition and thus cause residual polarization in the output. For example, mode-coupling centers located near the center or either end of the fiber can create optical paths for which optical components are in the different modes over a length less than the depolarization length, even though the fiber length is long compared to the depolarization length (Fig. 2). If made to interfere at the output, these optical components will then exhibit some degree of polarization. If the optical input is in a single polarization mode, we expect that mode coupling will tend to equalize power between the modes, after which the processes described above will determine the final degree of polarization. We now proceed to develop this picture mathematically. Our development is drawn largely

Manuscript received October 12, 1982; revised December 3, 1982.

W. K. Burns and R. P. Moeller are with the Naval Research Laboratory, Washington, DC 20375.

C.-L. Chen was on leave with the Naval Research Laboratory, Washington, DC 20375. He is with the School of Electrical Engineering, Purdue University, West Lafayette, IN 47907.

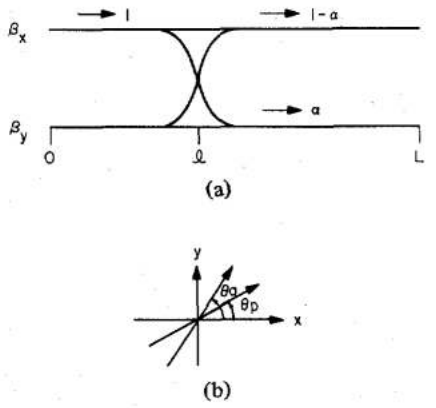

Fig. 1. (a) Model for a mode-coupling center which couples power α between the polarization modes. (b) Orientation of transmission axis of input polarizer and output analyzer with respect to fiber birefringence axes.

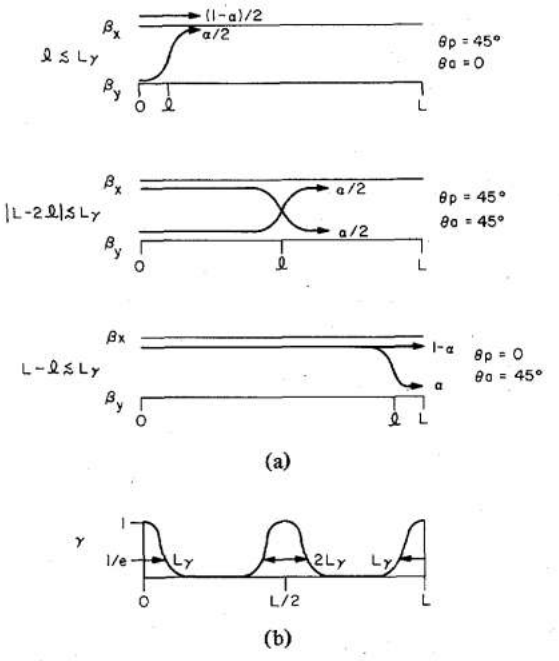

Fig. 2. (a) Models for mode-coupling centers at the beginning, middle, and end of the fiber that contribute to the degree of polarization. The polarizer and analyzer angles for which each case is maximized is also shown. l denotes the position of the mode-coupling center and L_γ is the depolarization length. (b) The corresponding values of the magnitude of the degree of coherence for each case in (a) when $L_\gamma \ll L$.

from the work of Sakai *et al.* [4], Born and Wolf [7], and Burns *et al.* [9], and generally follows the notation of Sakai's paper [4].

Consider a single-mode fiber with propagation constants β_x and β_y corresponding to the two polarization eigenmodes. We assume one discrete mode-coupling center, which couples a power α between the modes, at a position l along the fiber of length L (Fig. 1(a)). The transfer matrix for the coupling center is then given by

$$\begin{bmatrix} E_x(l^+) \\ E_y(l^+) \end{bmatrix} = \begin{bmatrix} \sqrt{1-\alpha} & \sqrt{\alpha} \\ -\sqrt{\alpha} & \sqrt{1-\alpha} \end{bmatrix} \begin{bmatrix} E_x(l^-) \\ E_y(l^-) \end{bmatrix} \tag{1}$$

where the superscripts $-$ and $+$ refer to positions immediately before and after the center, respectively. We assume a broadband source with unity power input is passed through a polarizer with its transmission axis at an angle θ_p from the mode axis X (Fig. 1(b)). The time-dependent electric field input to the fiber may then be represented

$$\begin{bmatrix} E_{0x}(t) \\ E_{0y}(t) \end{bmatrix} = \begin{bmatrix} \cos\theta_p \\ \sin\theta_p \end{bmatrix} e(t)\, e^{i\omega_0 t} \tag{2a}$$

where

$$\langle e(t)\, e^*(t) \rangle = 1. \tag{2b}$$

In (2), $\langle\ \rangle$ signifies time average and ω_0 is the source-center frequency.

Propagation in the fiber is governed by the frequency-dependent propagation constants $\beta_x \equiv \beta_x(\omega)$ and $\beta_y \equiv \beta_y(\omega)$. Employing the transfer matrix in (1) we can write the frequency-dependent fiber outputs as

$$\begin{bmatrix} E_x(\omega) \\ E_y(\omega) \end{bmatrix} = \begin{bmatrix} \sqrt{1-\alpha}\, e^{-i\beta_x L} & \sqrt{\alpha}\, e^{-i[\beta_y l + \beta_x (L-l)]} \\ -\sqrt{\alpha}\, e^{-i[\beta_x l + \beta_y (L-l)]} & \sqrt{1-\alpha}\, e^{-i\beta_y L} \end{bmatrix} \begin{bmatrix} E_{0x}(\omega) \\ E_{0y}(\omega) \end{bmatrix} \tag{3}$$

where $E_{0x}(\omega)$ and $E_{0y}(\omega)$ are the input fields at the frequency component ω. With an output analyzer with transmission axis at an angle θ_a from the X axis, the fiber output may be expressed

$$E(\omega) = E_x(\omega) \cos\theta_a + E_y(\omega) \sin\theta_a. \tag{4}$$

The output equations (3) and (4) are frequency dependent, whereas the input in (2) is time dependent. We require the time averaged output intensity

$$I = \langle |E(t)|^2 \rangle. \tag{5}$$

This problem may be treated by employing the rule for interference of quasi-monochromatic light [7], which we state here for the case of polarization modes in a dispersive medium [1], [9]. For an output frequency-dependent field of the form

$$E(\omega) = E_x(\omega)\, e^{-i\beta_x z} + E_y(\omega)\, e^{-i\beta_y z} \tag{6a}$$

where E_x and E_y have propagated in different modes but are now assumed to be polarized in the same direction, the output time averaged intensity is given by

$$I(z) = I_x + I_y + 2\sqrt{I_x I_y}\, \gamma(z) \cos \Delta\beta_0 z. \tag{6b}$$

Here I_x is the time averaged intensity $I_x = \langle |E_x(t)|^2 \rangle$, and similarly for I_y. z is the fiber length over which power is propagating in the two modes, and $\Delta\beta_0 = \beta_y(\omega_0) - \beta_x(\omega_0)$. $\gamma(z)$ is the degree of coherence [4], [7] which, for a source spectrum symmetric with respect to ω_0, is given by

$$\gamma(z) = \frac{\displaystyle\int_0^\infty |\nu(\omega)|^2 \cos[(\omega - \omega_0)\, \delta\tau_g z]\, d\omega}{\displaystyle\int_0^\infty |\nu(\omega)|^2\, d\omega} \tag{7}$$

where $|\nu(\omega)|^2$ is the source spectral intensity and $\delta\tau_g = d\Delta\beta/d\omega$ is the group-delay difference or polarization-mode dispersion. For a Gaussian spectrum defined by

$$|\nu(\omega)|^2 = \exp\left[-\ln 2\left(\frac{\omega-\omega_0}{\delta\omega}\right)^2\right]. \tag{8a}$$

Equation (7) becomes [4]

$$\gamma(z) = \exp\left[-\left(\frac{\delta\omega\delta\tau_g z}{2\sqrt{\ln 2}}\right)^2\right] \tag{8b}$$

where $2\delta\omega$ is the full spectral width at half maximum intensity. We note that $\gamma(z)$ varies between 0 and 1 and exponentially decays to e^{-1} at a length

$$L_\gamma = \frac{2\sqrt{\ln 2}}{\delta\omega\delta\tau_g} \tag{9}$$

which may be considered typical of the distance over which the light can propagate in the two modes and still interfere upon recombination. We will refer to L_γ as the depolarization length. In the narrow band limit ($\delta\omega \to 0$), we have $\gamma(z) \to 1$ so that (6) reduces to the usual result for monochromatic light.

Using this result we obtain the fiber output intensity $I(\theta_p, \theta_a)$ as a function of the polarizer and analyzer positions. With the polarizer parallel to the X axis ($\theta_p = 0$), the result is

$$I(0,\theta_a) = \cos^2\theta_a - \alpha\cos 2\theta_a - \sqrt{1-\alpha}\sqrt{\alpha}\sin 2\theta_a\gamma(L-l)\cos\Delta\beta_0(L-l). \tag{10a}$$

With the polarizer between the axes ($\theta_p = 45°$), the result is

$$I(45°,\theta_a) = \tfrac{1}{2} + \tfrac{1}{2}\sin 2\theta_a\left[(1-\alpha)\gamma(L)\cos\Delta\beta_0 L - \alpha\gamma(L-2l)\cos\Delta\beta_0(L-2l)\right] + \sqrt{1-\alpha}\sqrt{\alpha}\cos 2\theta_a\gamma(l)\cos\Delta\beta_0 l. \tag{10b}$$

We are interested in the case where the fiber length $L \gg L_\gamma$ so that $\gamma(L) \approx 0$. Then we see that interference terms occur in the output intensity which are caused by a mode-coupling center located such that $l \leqslant L_\gamma$, $|L-2l| \leqslant L_\gamma$, or $L-l \leqslant L_\gamma$, i.e., at the beginning, middle, or end of the fiber. When one of these conditions is satisfied, the corresponding $\gamma(z)$ is nonzero. We note that the presence of interference in the output implies a nonzero degree of polarization, since depolarized light cannot cause interference.

We can likewise calculate the degree of polarization [4] of the fiber output, using the model of a discrete mode-coupling center. The degree of polarization is calculated from the coherency matrix $\boldsymbol{J}$

$$\boldsymbol{J} = \langle E\cdot E^\dagger\rangle = \begin{bmatrix}\langle E_x E_x^*\rangle & \langle E_x E_y^*\rangle \\ \langle E_y E_x^*\rangle & \langle E_y E_y^*\rangle\end{bmatrix} \tag{11}$$

where $\dagger$ signifies the Hermitian transpose. The time varying field inputs may be expressed in terms of the envelope of the complex analytic signal [4] by defining $e(t)$ in 2(a) as

$$e(t) = 2\int_0^\infty \nu(\omega)\, e^{i(\omega-\omega_0)t}\, d\omega \tag{12}$$

which corresponds to input power $I_0 = \text{trace}\,(\boldsymbol{J}_0)$

$$I_0 = \langle E_{0x}(t)\,E_{0x}^*(t) + E_{0y}(t)\,E_{0y}^*(t)\rangle \tag{13a}$$

$$= 8\pi\int_0^\infty |\nu(\omega)|^2\, d\omega. \tag{13b}$$

To derive (13) Parseval's theorem is employed [7]. For our case, the output time-varying fields are expressed from (3) and Sakai *et al.* [4] and Burns *et al.* [9] as

$$E_x(t) = \cos\theta_p\sqrt{1-\alpha}\, e^{i(\omega_0 t-\beta_{x0}L)}\, e(t-\beta'_{x0}L) + \sin\theta_p\sqrt{\alpha}\, e^{i[\omega_0 t-\beta_{x0}(L-l)-\beta_{y0}l]} \cdot e(t-\beta'_{x0}(L-l)-\beta'_{y0}l) \tag{14a}$$

$$E_y(t) = -\cos\theta_p\sqrt{\alpha}\, e^{i[\omega_0 t-\beta_{x0}l-\beta_{y0}(L-l)]} \cdot e(t-\beta'_{x0}l-\beta'_{y0}(L-l)) + \sin\theta_p\sqrt{1-\alpha}\, e^{i(\omega_0 t-\beta_{y0}L)}\, e(t-\beta'_{y0}L) \tag{14b}$$

where β' denotes differentiation of β by ω. The degree of polarization is obtained from the coherency matrix as

$$P = \left[1 - \frac{4\,det\boldsymbol{J}}{(tr\boldsymbol{J})^2}\right]^{1/2} \tag{15}$$

which yields $P(\theta_p)$ as a function of the input polarization azimuth. For $\theta_p = 0$, we get

$$P(0) = \{1 - 4\alpha(1-\alpha)\,[1-\gamma^2(L-l)]\}^{1/2} \tag{16a}$$

and for $\theta_p = 45°$

$$P(45°) = \{4\alpha(1-\alpha)\cos^2\Delta\beta_0 l\,[\gamma^2(l) - \gamma(L)\,\gamma(L-2l)] + [(1-\alpha)\,\gamma(L) + \alpha\gamma(L-2l)]^2\}^{1/2} \tag{16b}$$

where $\gamma(z)$ is given in (7).

From (16) we see that with no mode coupling ($\alpha = 0$) we have $P(0) = 1$ and $P(45°) = \gamma(L)$, in agreement with (4). For $L \gg L_\gamma$ such that $\gamma(L) \approx 0$ we obtain the following results for particular values of α and l:

$$P(0) = \gamma(L-l), \qquad \alpha = \tfrac{1}{2} \tag{17a}$$

$$P(45°) \approx |\cos\Delta\beta_0 l|\,\gamma(l), \qquad \alpha = \tfrac{1}{2},\ l \leqslant L_\gamma \tag{17b}$$

or

$$P(45°) = \gamma(L-2l), \qquad \alpha = 1 \tag{17c}$$

For these simplifying choices for α the degree of polarization is either equal to, or proportional to, the degree of coherence associated with the location of the mode-coupling center. This result is in direct analogy with the result of $P(45°) = \gamma(L)$ when $\alpha = 0$. We see that the mode-coupling centers at particular positions along the fiber contribute to the degree of polarization, as we expected from the output equation (10). Since both the position and strength of the mode-coupling centers are likely to be effected by environmental perturbations, we would expect, in this limit, to see environmentally induced fluctuations in the degree of polarization. This effect is enhanced in (17b) where the interference term $\cos\Delta\beta_0 l$ occurs.

The mode-coupling centers may be viewed as effecting interference and degree of polarization by providing paths

through the fiber, for part of the light, for which the group-delay difference between the interfering components is less than the coherence time [1]. Expressed in terms of lengths, the output will show a nonzero P if the path length over which the interfering components are in different modes is $\leqslant L_\gamma$. We illustrate these paths for the contributing centers in Fig. 2(a) and sketch the corresponding value of γ (assuming $L \gg L_\gamma$) associated with each region in Fig. 2(b).

So far we have considered only one discrete mode-coupling center, an assumption which is undoubtedly unrealistic. Although we cannot mathematically handle multiple-mode-coupling centers is mixing of the polarization modes [5], [6], Aside from depolarization, the primary effect of multiple-mode-coupling centers is mixing of the polarization modes [5], [6] a process that is characterized by coupled power theory by length $1/h$. This is the characteristic length in which input power in one mode becomes evenly divided between both. We note from our previous considerations that light which is coupled between modes at two positions along the fiber will become depolarized if either position is not one of the allowed positions as shown in Fig. 2. Multiple-mode-coupling processes then are not likely to make a substantial contribution to a nonzero degree of polarization.

When the incident light azimuth is between the fiber birefringence axes ($\theta_p = 45°$), the power is already equally divided between the polarization modes. The degree of polarization is governed by (16b). For $L \leqslant L_\gamma$ we expect to see P decrease as $\gamma(L)$, with mode coupling not playing a major role. For $L_\gamma \leqslant L \leqslant 4L_\gamma$ mode-coupling centers become important in determining P. The length of fiber with contributing mode-coupling centers is increasing in this regime. For $L \geqslant 4L_\gamma$, the length of fiber with contributing centers saturates at $\sim 3L_\gamma$, since only the beginning and middle sections contribute. Additional fiber length only changes the position of the contributing centers at the middle of the fiber. We would expect P to reach an approximately constant level ($P_\infty(45°)$).

Next we consider the case of incident-light azimuth parallel to a birefringence axis ($\theta_p = 0$). From (16a) we see that, without mode coupling, $P = 1$ independent of length. In this case, mode-coupling centers, independent of position, tend to degrade P from $1 \rightarrow 0$. For example, a center with $\alpha = 1/2$ at a position $L - l > L_\gamma$ yields $P = 0$. However, mode-coupling centers at the end of the fiber ($L - l \leqslant L_\gamma$) leads to interference and a nonzero P. For $L < 1/h$, power is being equalized between the modes by mode coupling, and we expect P to be a measure of the fraction of power in the input channel (X) that has not coupled to the Y channel. This may be expressed as

$$P \sim \frac{I_x - I_y}{I_t} = \frac{2I_x}{I_t} - 1 \sim e^{-2hL} \tag{18}$$

where $I_t = I_x + I_y$ and we have employed the result of the work of Rashleigh *et al.* [6]. For $L > 1/h$, P is determined by mode coupling at the end of the fiber, and we expect P to again reach an approximately constant value ($P_\infty(0)$). We adapt (18) to reflect this effect and obtain the phenomenological equation

$$P(0) = P_\infty(0) + (1 - P_\infty(0))\, e^{-2hL}. \tag{19}$$

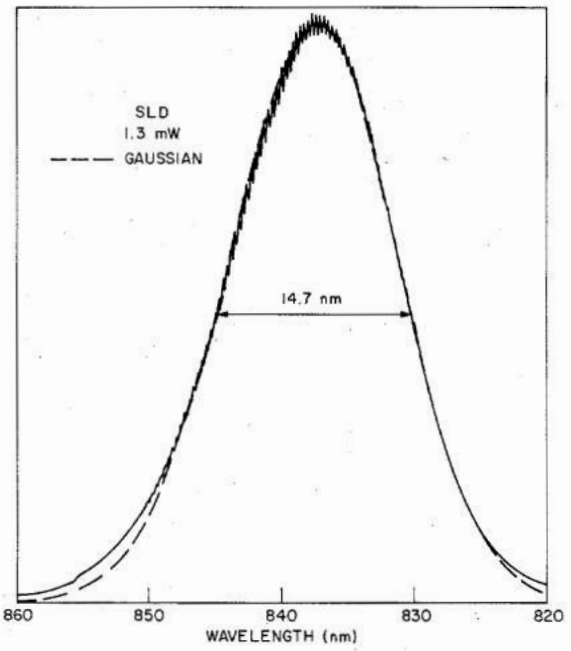

Fig. 3. Superluminescent diode spectrum with Gaussian fit.

III. Experiment and Discussion

To test the model just developed we measured the degree of polarization in various lengths of single-mode fiber with a broad-band source. The source was a superluminescent diode developed by General Optronics [8] which had sufficiently narrow divergence to couple 50–100 μW into the single-mode fiber. The fiber was Corning single-mode fiber #505604. It was a 1.1-km piece with a core diameter of 4 μm, a NA of 0.1, and an attenuation of 3.6 dB/km. The source was passed through a polarizer before input to the fiber and the output was analyzed with a Soleil–Babinet compensator and an analyzer. Degree of polarization is given by [7]

$$P = \frac{I_{\max}(\theta_a, \epsilon) - I_{\min}(\theta_a, \epsilon)}{I_{\max}(\theta_a, \epsilon) + I_{\min}(\theta_a, \epsilon)} \tag{20}$$

where $I_{\max}(\theta_a, \epsilon)$ and $I_{\min}(\theta_a, \epsilon)$ are the maximum and minimum observed intensities for all possible delays introduced by the compensator (ϵ) and all possible orientations of the analyzer. The fiber was wound on a drum of 15-cm diam and care was taken to hold the fiber ends without introducing additional birefringence. The fiber ends were suitably mode stripped.

The source spectrum at 1.3-mW output is shown in Fig. 3 with a Gaussian fit from (7). Due to the slight asymmetry of the output we use an asymmetric fit which yields an average half-width $\delta\lambda = 7.4$ nm and a center wavelength $\lambda_0 = 838$ nm. The corresponding frequency half-width is $\delta\omega = 19.7$ rad/ps. Although the Gaussian fit is not perfect, we assume it to be sufficiently good for our purposes to employ the Gaussian result for γ in (8b). Typical data for the degree of polarization for our longest (1.1 km) and shortest (1.3 m) length is shown in Fig. 4. These two results were taken with a single constant input condition. The short length result clearly shows that the fiber birefringence axes occur at input angles near

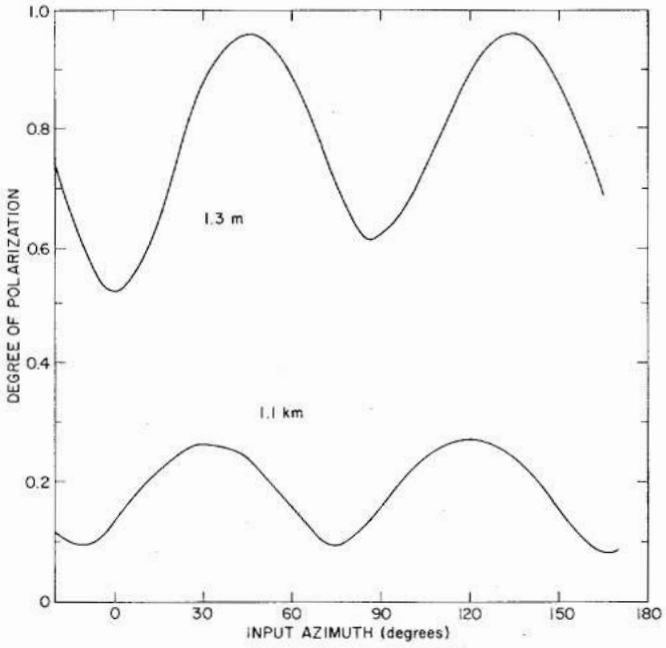

Fig. 4. Degree of polarization versus input azimuth (relative to lab frame) for shortest and longest length of single-mode fiber investigated.

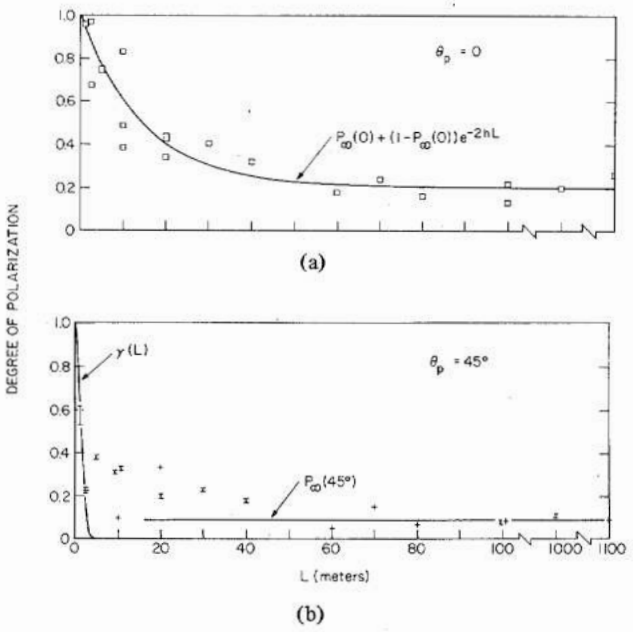

Fig. 6. Degree of polarization data versus fiber length when input azimuth is (a) on fiber birefringence axis ($\theta_p = 0$), and (b) between fiber birefringence axes ($\theta_p = 45°$).

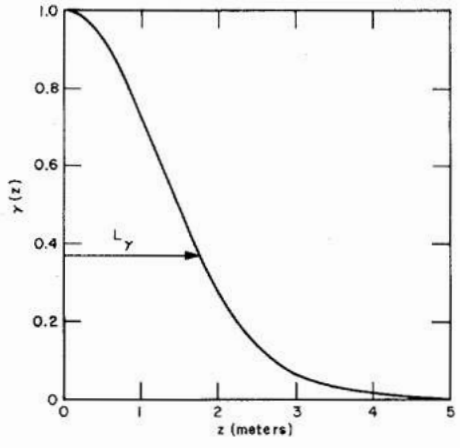

Fig. 5. Magnitude of the degree of coherence versus propagation length for the source and fiber used in our experiments.

45 and 135°, since we expect the least depolarization to occur on axis for a short length. The minima P between these axes ($\theta_p = 45°$) can be used to calculate the group-delay difference $\delta\tau_g$ for our fiber. Using (16b) in the no mode-coupling limit ($\alpha = 0$) and (8b) for $\gamma(L)$ we obtain $\delta\tau_g = 47$ ps/km. We then plot $\gamma(z)$ in Fig. 5 and calculate the depolarization length L_γ from (9) to be 1.8 m.

Most of our data for P was taken by cutting back on a fiber with an initial length of 100 m, without changing the input conditions. We summarize all our data in Fig. 6 for $\theta_p = 0$ and $\theta_p = 45°$. We see that for $\theta_p = 0$ a good fit to (19) could be obtained with $1/h = 30$ m. Considerable variation was observed between measurements on separate, but identical, lengths of fiber as at 2.5, 10, and 20 m. Somewhat less variation was observed for separate measurements on the same piece of fiber, as at 100 m. These observations are consistent with the coupling-center model, since different pieces of fiber would have different coupling-center distributions, and because even on the same length of fiber the strength of the centers can be environmentally effected. A surprising result was that P at ~1 km was essentially the same as P at 100 m.

The data at $\theta_p = 45°$ is shown in Fig. 6(b). We attempt a fit to $\gamma(L)$ at short lengths and to a constant value $P_\infty(45°)$ at long lengths. Again, we observe that P at 1 km is very much like P at 100 m. The fit to $\gamma(L)$ is sketchy since the measurement at 1.3 m was used to derive $\gamma(L)$ and there are only two independent points at 2.5 m. At 5 m, P clearly increases above the prediction of $\gamma(L)$, showing the effect of mode coupling in the fiber. Our model predicted saturation after $4L_\gamma$ or ~10 m, but the data seems to fall more slowly until $P_\infty(45°)$ is reached. This could be due to fluctuations in the measurement or inadequacy of the model to account for multiple coupling centers.

We note that, to our knowledge, the measurement reported here is the first measurement of $1/h$, the characteristic length for polarization-mode mixing, on a nominally isotropic fiber. Our measurement technique is closely related to that used for high birefringence fibers [6]. We were also able to measure this fiber's birefringence beat length $L_p = 2\pi/(\beta_x - \beta_y)$ by aligning our input at $\theta_p = 45°$ and measuring the period of the variation of the visibility [5] as the fiber length was cut back. The measured beat length was ~14 cm.

A difficulty in interpretation of our data lay in the identification of the birefringence axes for data corresponding to fiber lengths $\gg 1/h$. For example, in Fig. 4 axis identification is obvious at 1.3 m, but at 1.1 km we do not know whether the peaks or the valleys of P correspond to the birefringence axes. We no longer get a clue from the distribution of power between the polarization modes since that power is essentially balanced after $1/h$ or 30 m. We do not know whether $P_\infty(0)$ is greater or less than $P_\infty(45°)$, or whether fluctuations might cause

these quantities to interchange. However, the effect of the axes was evident, even after 1.1 km of propagation, and $P_\infty(0)$ and $P_\infty(45^\circ)$ were not observed to be the same. Since the data in Fig. 4 was taken with a single input condition, the near alignment of the peaks between the data corresponding to each length is suggestive that the peaks of the 1.1-km data could be identified with the axes as are the peaks of the 1.3-m data. However, when the 100-m length was cut back we observed the peak position to wander some ±30–35° from the mean position, which does not allow for a conclusive identification. In identification of the data for Fig. 5 we made what seemed the most reasonable choice and continued to identify the peaks of $P(\theta_p)$ with $P(0)$ as L increased beyond $1/h$.

Our observation of axis wander mentioned above is significant because it implies that the orientation of the axes varies with position along the fiber. This is not surprising as the fiber's birefringence is presumably due to randomly induced strains and geometric distortions. It means that the model developed, which assumes a fixed orientation of birefringence axes, must be applied with caution. For example, this could account for the somewhat poor fit of experiment to theory in Fig. 6(b) between 10 and 40 m.

Perhaps the most interesting observation of our experiments was that the degree of polarization was maintained, essentially undiminished, between lengths of 50–100 m out to 1.1 km, a length much longer than the mode mixing length $1/h$. One might expect that multiple-mode-coupling processes would reduce the amount of power capable of interfering coherently at the end of the fiber, and thus cause an eventual reduction in the degree of polarization.

IV. Conclusions

We have used a mode-coupling-center model to account for depolarization of the broad-band source in a single-mode optical fiber with ordinary birefringence. Experimental results are presented and are substantially accounted for by the model developed. The degree of polarization in long lengths of fiber is determined by mode coupling that occurs at specific sites at the beginning, middle, and end of the fiber. We would expect, and have observed, the resulting degree of polarization to be susceptible to environmental fluctuations. The degree of polarization has been shown to remain essentially constant over lengths of fiber from 100 m to 1 km long. We expect these results to be of interest in applications where depolarization or the lack of it results in system noise, i.e., coherent communications and fiber-optical gyroscopes. Although higher birefringence fiber will reduce many of the effects observed here, ultimate system noise due to the degree of polarization will still derive from the mechanisms described.

References

[1] S. C. Rashleigh and R. Ulrich, "Polarization mode dispersion in single-mode fibers," *Opt. Lett.*, vol. 3, p. 60, 1978.

[2] K. Bohm, P. Marten, K. Petermann, E. Weidel, and R. Ulrich, "Low drift fiber gyro using a superluminescent diode," *Electron. Lett.*, vol. 17, p. 352, 1981.

[3] W. K. Burns, R. P. Moeller, and C. A. Villarruel, "Observation of low noise in a passive fiber gyroscope," *Electron. Lett.*, vol. 18, p. 648, 1982.

[4] J. I. Sakai, S. Machida, and T. Kimura, "Degree of polarization in anisotropic single-mode optical fibers: Theory," *IEEE J. Quantum Electron.*, vol. QE-18, p. 488, 1982.

[5] I. P. Kaminov, "Polarization in optical fibers," *IEEE J. Quantum Electron.*, vol. QE-17, p. 15, 1981.

[6] S. C. Rashleigh, W. K. Burns, R. P. Moeller, and R. Ulrich, "Polarization holding in birefringent single-mode fibers," *Opt. Lett.*, vol. 7, p. 40, 1982.

[7] M. Born and E. Wolf, *Principles of Optics*, 3rd ed. New York: Pergamon, 1965, pp. 491–506, 544–554.

[8] C. S. Wang, W. H. Cheng, C. J. Hwang, W. K. Burns, and R. P. Moeller, "High power low divergence super radiance diode," *Appl. Phys. Lett.*, vol. 41, p. 587, 1982.

[9] W. K. Burns, C. L. Chen, and R. P. Moeller, "Fiber optic gyroscope with broad-band sources," pp. 98–105, this issue.

*

William K. Burns (M'80) was born in Philadelphia, PA, in June 1943. He received the B.S. degree in engineering physics from Cornell University, Ithaca, NY, in 1965, and the M.S. and Ph.D. degrees in applied physics from Harvard University, Cambridge, MA, in 1967 and 1971, respectively. His thesis research was in nonlinear optics.

During 1971 he was a staff member at Arthur D. Little, Inc., Cambridge, MA, where he contributed to various laser-related studies and surveys. Since 1972 he has been a Research Physicist at the Naval Research Laboratory, Washington, DC. He is presently Head of the Optical Waveguide Section of the Optical Techniques Branch. His research interests include integrated optics, single-mode fiber optics, and the application of single-mode technology to communications, sensors, and signal processing.

Dr. Burns is a member of the Optical Society of America.

*

Robert P. Moeller was born on January 26, 1947. He received the B.S. and M.S. degrees in physics from John Carroll University, Cleveland, OH, in 1969 and 1971, respectively.

In 1972, on a Presidential Internship, he set up a laser schlieren photographic system at the Naval Research Laboratory, Washington, DC, for the visualization of underwater acoustic wares and a stabilized multipass Fabry–Pérot. At Catholic University of America's Vitreous State Laboratory, he measured viscoelastic properties of lubricants using laser light scattering digital autocorrelation and Fabry–Perot techniques. Since March of 1978 he has been with the Naval Research Laboratory characterizing single-mode optical fibers, couplers, and integrated optical modulators and switches.

*

Chin-Lin Chen received the B.S.E.E. degree from National Taiwan University, Taipei, China, in 1958, the M.S. degree from North Dakota State University, Fargo, in 1961, and the Ph.D. degree from Harvard University, Cambridge, MA, in 1965.

From 1965 to 1966, he was a Research Fellow in the Division of Engineering and Applied Physics, Harvard University. In 1966, he joined the School of Electrical Engineering, Purdue University, West Lafayette, IN, as an Assistant

Professor. He is currently a Professor of Electrical Engineering. From 1981 to the present he has been on sabbatical leave at the Vitreous State Laboratory, The Catholic University of America, Washington, DC, and the Naval Research Laboratory, Washington, DC. His research interests are in the areas of scattering and diffraction of electromagnetic waves, antenna radiation, surface acoustic wave filters and cavities, and the integrated and fiber-optical components.

Dr. Chen is a member of Sigma Xi, Eta Kappa Nu, the American Society for Engineering Education, and the U.S. National Committee for the International Union of Radio Science.

Transmission-Loss Characteristics of Al_2O_3-Doped Silica Fibers

YASUJI OHMORI, TETSUO MIYA, AND MASAHARU HORIGUCHI

Abstract—**Transmission-loss characteristics of Al_2O_3-doped silica fibers have been investigated to develop an Al_2O_3 alternative dopant for VAD silica-based optical fibers. Optical properties of Al_2O_3-doped silica bulk glass and fibers were measured in the 0.11–30-μm spectral region. From the experimental results, the intrinsic loss due to glass material was estimated for Al_2O_3-doped silica fibers. The calculated intrinsic loss minima for Al_2O_3-doped silica fibers with 0.2- and 1.0-percent relative refractive-index differences were 0.17 dB/km at 1.548 μm and 0.28 dB/km at 1.565 μm, respectively.**

I. Introduction

GERMANIUM OXIDE is most widely used as a dopant in low-loss silica-based optical fibers to raise the refractive index. However, there are problems in regard to stable germanium availability and cost in the future. Recently, several investigations have been made to develop dopants alternative to GeO_2 [1], [2]. Among many candidates for the alternative dopants, Al_2O_3 is considered most promising because aluminum has many advantages in cost, long-term availability, and purification. Also, alumina has no absorption peak in the visible and the near-infrared wavelength region.

The authors reported that a 0.65-dB/km low-loss value at 1.56 μm had been attained with Al_2O_3-doped single-mode fibers fabricated by the VAD process [3]. This success confirms that Al_2O_3 is competitive with GeO_2 in low-loss fiber characteristics. The transmission-loss characteristics of silica-based fibers depend on the kind of dopant used. In order to design fiber characteristics, many investigations have been made about the influence of conventional dopants, such as GeO_2, P_2O_5 and B_2O_3, on fiber transmission loss [4]–[12]. Then, the transmission-loss characteristics of Al_2O_3-doped silica fibers are highly desirable to develop the Al_2O_3 alternative dopant for VAD silica-based optical fibers.

This paper describes transmission-loss characteristics of Al_2O_3-doped silica fibers. The intrinsic loss due to glass material in the visible and the near-infrared wavelength region, which is composed of ultraviolet absorption, infrared absorption, and Rayleigh scattering was determined from Al_2O_3-doped bulk-glass samples and Al_2O_3-doped silica fibers, and was compared with that for GeO_2-doped silica fibers. Spectral loss of low-loss Al_2O_3-doped silica fibers, which were fabricated by the VAD process, was also classified by the loss factors.

Manuscript received September 16, 1982; revised November 1982

The authors are with the Ibaraki Electrical Laboratory, Nippon Telegraph and Telephone Public Corporation, Ibaraki-ken 319-11, Japan.

II. Experimental Procedures

A. Sample Preparation

Optical fibers consisting of Al_2O_3-SiO_2 core and SiO_2 cladding, and Al_2O_3-doped silica bulk-glass samples were prepared by the VAD process. Basic apparatus for the VAD system and the key points for preparing high-quality Al_2O_3-doped silica glass are described in detail in a previous letter [3]. To investigate ultraviolet and infrared optical properties of Al_2O_3-SiO_2 glass, Al_2O_3-doped silica bulk-glass samples were prepared with up to 0.54 percent in relative refractive-index difference. Three kinds of low-loss optical fibers were fabricated in order to clarify basic loss characteristics of Al_2O_3-doped silica fibers in the visible and the near-infrared region. One was multi-mode step-index fiber and the others were single-mode fibers. The relative refractive-index differences between core and cladding were 0.1 and 0.3 percent for the single-mode fibers and 1.0 percent for the multi-mode fiber. These transmission loss characteristics are illustrated in the papers by Ohmori *et al.* [3] and Ohmori and Nakahara [13]. They are also discussed in Section III-C from the viewpoint of loss analysis.

B. Measurement Procedures

Ultraviolet optical properties of Al_2O_3-SiO_2 glass were measured with conventional ultraviolet spectroscopy in the wavelength region between 0.11–0.25 μm. UV reflectance spectra were obtained on mechanically polished samples in the 0.11–0.16-μm wavelength region. UV transmittance spectra were obtained on mechanically polished plate samples of various thicknesses in the 0.16–0.25-μm wavelength region.

0733-8724/83/0300-0050$01.00